Data in Brief 6 (2016) 550–555

Contents lists available at ScienceDirect

Data in Brief

journal homepage: www.elsevier.com/locate/dib

Data Article

Structural basis of specific inhibition of tissue-type plasminogen activator by plasminogen activators inhibitor-1

Lihu Gong [a,b], Min Liu [a,b], Tu Zeng [a], Xiaoli Shi [a], Cai Yuan [a], Peter A. Andreasen [c], Mingdong Huang [a,b,*]

[a] State Key Laboratory of Structural Chemistry, Danish-Chinese Centre for Proteases and Cancer, Fujian Institute of Research on the Structure of Matter, Chinese Academy of Sciences, Fuzhou, Fujian 350002, China

[b] University of Chinese Academy of Sciences, Beijing 100049, China

[c] Danish-Chinese Centre for Proteases and Cancer, Department of Molecular Biology and Genetics, Aarhus University, 8000 Aarhus C, Denmark

ARTICLE INFO

Article history:
Received 17 October 2015
Received in revised form
2 December 2015
Accepted 29 December 2015
Available online 6 January 2016

Keywords:
Tpa
Serine protease
PAI-1
Serpin
Michaëlis complex
Crystal structure
Fibrinolysis
Thrombolytic agents
Structural biology

ABSTRACT

Thrombosis is a leading cause of death worldwide [1]. Recombinant tissue-type plasminogen activator (tPA) is the FDA-approved thrombolytic drug for ischemic strokes, myocardial infarction and pulmonary embolism. tPA is a multi-domain serine protease of the trypsin-family [2] and catalyses the critical step in fibrinolysis [3], converting the zymogen plasminogen to the active serine protease plasmin, which degrades the fibrin network of thrombi and blood clots. tPA is rapidly inactivated by endogenous plasminogen activators inhibitor-1 (PAI-1) [4] (Fig. 1). Engineering on tPA to reduce its inhibition by PAI-1 without compromising its thrombolytic effect is a continuous effort [5]. Tenecteplase (TNK-tPA) is a newer generation of tPA variant showing slower inhibition by PAI-1 [6]. Extensive studies to understand the molecular interactions between tPA and PAI-1 have been carried out [7–18], however, the precise details at atomic resolution remain unknown. We report the crystal structure of tPA · PAI-1 complex here. The methods required to achieve these data include: (1) recombinant expression and purification of a PAI-1 variant (14-1B) containing four mutations (N150H, K154T, Q319L, and M354I), and a tPA serine protease domain (tPA-SPD) variant with three mutations (C122A, N173Q, and S195A, in the chymotrypsin numbering) [19]; (2) formation of a tPA-SPD · PAI-1 Michaëlis

* Corresponding author.
E-mail address: mhuang@fjirsm.ac.cn (M. Huang).

http://dx.doi.org/10.1016/j.dib.2015.12.050

complex in vitro [19]; and (3) solving the three-dimensional structure for this complex by X-ray crystallography [deposited in the PDB database as 5BRR]. The data explain the specificity of PAI-1 for tPA and uPA [19,20], and provide structural basis to design newer generation of PAI-1-resistant tPA variants as thrombolytic agents [19].

Specifications table

Subject area	*Biology*
More specific subject area	*Protein structure and biochemistry*
Type of data	*X-ray crystal structure, Mass spectrometry*
How data was acquired	*X-ray diffraction data were collected at Shanghai Synchrotron Radiation Facility. Mass spectra of MALDI-TOF-MS were obtained on a Bruker REFLEX III MALDI-TOF-MS (Bruker-Franzen, Bremen, Germany).*
Data format	*Processed*
Experimental factors	*Recombinant proteins were purified to high homogeneity before use.*
Experimental features	*The structure of the tPA · PAI-1 complex was determined by X-ray crystallography.*
Data source location	*City, Country and/or Latitude & Longitude (& GPS coordinates) for collected samples/data if applicable*
Data accessibility	*The data is available from the related publication by Gong et al. (http://www.ncbi.nlm.nih.gov/pubmed/26324706), and the structure deposited in the Protein Data Bank (entry 5BRR).*

Value of the data

- Determines the crystal structure of the Michaëlis complex between tPA and PAI-1.
- Provides insight on the specificity of PAI-1 for tPA and uPA.
- Identifies key residues of tPA for binding to PAI-1.
- Explains the PAI-1-resisting property of Tenecteplase.
- Offers important clues to design newer generation of PAI-1-resistant tPA variants.

1. Data, experimental design, materials and methods

1.1. Data and experimental design

We have determined the structure of tPA · PAI-1 Michaëlis complex and identified key residues of tPA for binding to PAI-1 by X-ray crystallography, and the data are summarized in the original publication [19].

We expressed the recombinant PAI-1 variant 14-1B (N150H, K154T, Q319L, and M354I) [21], using the expression vector pT7-PL and BL21 cells as soluble protein [22]. The choice of this particular variant is to obtain PAI-1 in active form, advantageous for crystallization, because the wild type PAI-1

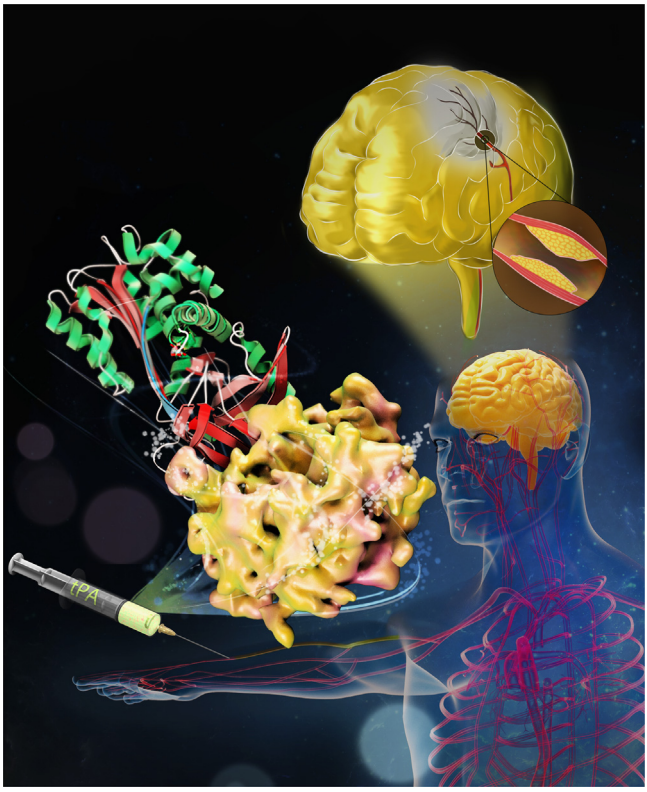

Fig. 1. A structural basis to design newer thrombolytics. Recombinant tPA (surface) is the FDA-approved thrombolytic drug. High dose of recombinant tPA is typically needed to lyse clot in stroke patients, partly due to its rapid inactivation by endogenous inhibitor (PAI-1, in ribbon). Such high dosage leads to dangerous side effects, including intracranial hemorrhage and neurotoxicity. Here, the crystal structure of tPA●PAI-1 Michaëlis complex was determined. This structure offers important clues to design newer generation of tPA thrombolytics with reduced PAI-1 inactivation.

has a half life of only 2 h and has propensity to spontaneously convert into an inactive, so-called latent form, and to aggregate at high concentration [23,24].

PAI-1 inhibits tPA by a suicide-substrate mechanism common to all SERPIN members [23,25] – see Fig. 1A in the original publication [19]. In this SERPIN mechanism, a long flexible loop of PAI-1 (reaction center loop, or RCL) inserts into the active site of tPA to form a transient Michaëlis complex. The RCL is cleaved by tPA through the classical serine proteolytic mechanism. tPA forms a covalent acyl-enzyme intermediate with PAI-1 by cleaving the scissible bond of PAI-1 RCL, following the Michaëlis complex. Before the hydrolysis of this acyl-enzyme intermediate, the PAI-1 RCL undergoes major conformational changes and inserts itself into the PAI-1 β-sheet A. At the same time, the tPA in the intermediate is pulled to the other side of PAI-1, distorted, and deactivated before the hydrolysis of the acyl-enzyme intermediate can take place.

Human tPA contains a fibronectin type II domain (amino acids 1–50), a growth factor domain (amino acids 51–91), two kringle domains (amino acids 92–261), an interdomain linker (amino acids 262–275) and a serine protease domain (SPD, amino acids 276–527) [2] – see Fig. 1B in the original publication [19]. The tPA-SPD is the catalytic domain responsible for the plasminogen activation and is inhibited by PAI-1. Thus, we used only the recombinant tPA-SPD domain to form the Michaëlis complex with PAI-1. We generated three mutations in tPA-SPD: S478A (or S195A in the chymotrypsin numbering) to render the tPA-SPD catalytically inactive, so the Michaëlis complex does not proceed to a stable, covalent complex; N448Q (or N173Q in the chymotrypsin numbering) to remove the glycosylation on tPA-SPD, increasing the homogeneity of the recombinant protein and facilitating

Table 1
Trypsin digested fragments of recombinant tPA-SPD SPD from MALDI-TOF-MS and the expected fragment mass.

Mr observed (Da)	Mr calculated (Da)	Peptide sequence
1387.1	1386.8004	^{53}FPPHHLTVILGR^{64}
1335.8	1335.6328	^{142}HEALSPFYSER^{152}
1179.4	1179.6157	^{239}VTNYLDWIR^{247}
878.8	878.4618	^{231}DVPGVYTK^{238}
722.4	722.3831	^{160}LYPSSR^{165}

protein crystallization; and C395A (or C122A in the chymotrypsin numbering that will be used throughout the rest of text) mutation to remove the disulfide bond linked to K2 domain – see Fig. 1B in the original publication [19]. The recombinant tPA-SPD mutant was expressed in *P. pastoris* and confirmed by SDS-PAGE and mass spectrometry after trypsin digestion (Table 1).

The recombinant PAI-1 14-1B and tPA-SPD were respectively dialysed into a high-concentration salt (1 M NaCl) and low pH (20 mM Mes pH 6.1) buffer before the Michaëlis complex formation. This condition is required to stabilize PAI-1 at its active form. Subsequently, these two proteins in high salt concentrations and low pH buffer were mixed in a 1:1 M ratio, followed by a dialysis into a low-concentration salt (150 mM NaCl) and neutral pH (20 mM Tris–HCl pH 7.4) buffer. This dialysing step ensures the complex formation similar to that in physiologic condition. A further gel filtration chromatography purification yielded a complex of greater than 99% purity.

2. Materials and methods

2.1. Recombinant protein production

The recombinant PAI-1 mutant 14-1B [21] containing four point mutations (N150H, K154T, Q319L, and M354I), and a hexa-His-tag was expressed in *E. coli*, using the expression vector pT7-PL and BL21 cells as previously described [22]. The recombinant tPA-SPD was expressed in *P. pastoris* X-33. This strain facilitates the formation of five disulfide bonds (C42-C58, C50-C111, C100-C182, C136-C201, C168-C182 in chymotrypsin numbering) in tPA-SPD with a high yield about 50 mg recombinant protein per liter medium – see in the original publication [19].

2.2. The peptide mass fingerprinting of tPA-SPD by MALDI-TOF mass spectrometry

The SDS-PAGE was performed using 15% polyacrylamide gels. Following SDS-PAGE, the gels were stained with 0.1% (w/v) Coomassie brilliant blue R-250 in 25% (v/v) ethanol and 10% (v/v) acetic acid. The gel digestion was performed using a modified version of previously published protocol [26]. Briefly, the gel band containing 100 ng tPA-SPD was excised from the 15% two-dimensional SDS-PAGE gel, cut in pieces, and destained by washing with 50% (v/v) acetonitrile in 100 μl of 25 mM NH_4HCO_3 for 30 min at room temperature. The gel pieces were then dried in a SpeedVac Vacuum (Savant Instruments, Holbrook, NY, USA) and rehydrated at 4 °C for 15 min in 3–5 μl digestion solution (25 mM NH_4HCO_3 and 12.5 ng/μl modified sequence-grade trypsin). Then 3–5 μl of digestion solution without trypsin was added to keep the gel pieces wet during the digestion. After overnight incubation at 37 °C, the digestion was stopped with 5% trifluoroacetic acid (TFA) for 20 min. The peptides were extracted by 20 μl of 5% TFA for 1 h at 37 °C and then by 20 μl of 2.5% TFA/50% acetonitrile for 1 h at 37 °C. The combined supernatants were evaporated in the SpeedVac Vacuum and dissolved in 4 μl 0.5% aqueous TFA for MS analysis.

All mass spectra of MALDI-TOF-MS were obtained on a Bruker REFLEX III MALDI-TOF-MS (Bruker–Franzen, Bremen, Germany) in positive ion mode at an accelerating voltage of 20 kV with the matrix of α-cyano-4-hydroxy cinnamic acid. The spectra were internally calibrated using trypsin autolysis products. The peptide mass fingerprinting obtained was used to search through the SWISS-PROT and NCBI database by the Mascot search engine (http://mascot.proteomics.com.cn/) with a tolerance of $\sim +0.3$ D and one missed cleavage site.

2.3. X-ray crystallography

The tPA-SPD · PAI-1 Michaëlis complex was formed by mixing tPA-SPD and PAI-1 in a 1:1 M ratio at low concentration (~ 0.5 mg/ml), followed by dialysis into 20 mM Tris–HCl pH 7.4, and 150 mM NaCl, concentration to 0.5 ml volume for a further gel filtration chromatography purification, which yielded to a complex of greater than 99% purity. The purified complex was then concentrated to 10 mg/mL before setting up crystallization trials. Crystals of the tPA-SPD · PAI-1 Michaëlis complex were grown at 20 °C with the sitting drop method by mixing equal volumes of protein solution and precipitant solution (8% PEG-6000 and 0.1 M Tris pH 7.4), and appeared quickly within one day. However, the crystals always appeared as very thin plates, and decayed rapidly in the X-ray beam, posing great difficulty for X-ray data collection. Most crystals diffracted to only 4–5 Å at Shanghai Synchrotron Radiation Facility (SSRF) BL-17U beam line, and the diffracting spots often appeared as elongated or splitted shapes. After many crystallization and data collection trials for one and half years, one 3.16 Å data set was finally obtained at SSRF beam line BL17U using 25% glycerol as cryoprotectant at a wavelength of 0.979 Å. The data were processed and scaled using the HKL2000 program package [27]. The crystal belongs to $P2_12_12_1$ space group with one complex in the crystallographic asymmetric unit. The structure of the tPA-SPD · PAI-1 Michaëlis complex was solved by molecular replacement method using MolRep program [28], which gave very strong and unambiguous solutions. A tPA-SPD molecule was first positioned inside the crystal lattice using the structure of the tPA-SPD catalytic domain (PDB code 1A5H) [29] as a searching model and all the X-ray data up to 3.3 Å. The molecular replacement using MolRep gave a contrast of 12.33, a signal to sigma ratio for translational function of 16.02, and a correlation coefficient of 0.365. Next, the position of PAI-1 was searched using the model of active stable variant of PAI-1 (Protein Data Bank code 1DVM) [30] while fixing the already positioned tPA-SPD model, giving only one translational function with a signal to sigma ratio of 19.4, and a correlation coefficient of 0.538. The molecular replacement model was subjected to iterative refinement and manual model rebuilding using Refmac [31] and Coot [32], respectively, giving a final R factor and R_{free} factor of 0.20 and 0.27, respectively. The structure was validated with PROCHECK [33] and analyzed by PyMOL [34] and PISA [35]. The final refined crystal structure of tPA-SPD · PAI-1 Michaëlis complex was deposited in PDB with the code *5BRR*.

Acknowledgment

We thank the Shanghai Synchrotron Radiation Facility for the X-ray beam time and the scientists at beamline BL17U for assistance with X-ray data collection. This work was supported by Grants from the National Natural Science Foundation of China (31170707, 31370737) and CAS/SFEA International Partnership Program for Creative Research Teams.

Appendix A. Supplementary material

Supplementary data associated with this article can be found in the online version at http://dx.doi.org/10.1016/j.dib.2015.12.050.

References

[1] G.E. Raskob, P. Angchaisuksiri, A.N. Blanco, H. Buller, A. Gallus, B.J. Hunt, et al., Thrombosis: a major contributor to global disease burden, Thromb. Res. 134 (2014) 931–938.
[2] D. Pennica, W.E. Holmes, W.J. Kohr, R.N. Harkins, G.A. Vehar, C.A. Ward, et al., Cloning and expression of human tissue-type plasminogen-activator Cdna in *Escherichia coli*, Nature 301 (1983) 214–221.
[3] D. Collen, H.R. Lijnen, Molecular-basis of fibrinolysis, as relevant for thrombolytic therapy, Thromb. Haemost. 74 (1995) 167–171.

[4] J. Keijer, M. Linders, A.J. van Zonneveld, H.J. Ehrlich, J.P. de Boer, H. Pannekoek, The interaction of plasminogen activator inhibitor 1 with plasminogen activators (tissue-type and urokinase-type) and fibrin: localization of interaction sites and physiologic relevance, Blood 78 (1991) 401–409.
[5] D.B. Baruah, R.N. Dash, M.R. Chaudhari, S.S. Kadam, Plasminogen activators: a comparison, Vasc. Pharmacol. 44 (2006) 1–9.
[6] B.A. Keyt, N.F. Paoni, C.J. Refino, L. Berleau, H. Nguyen, A. Chow, et al., A faster-acting and more potent form of tissue plasminogen activator, Proc. Natl. Acad. Sci. USA 91 (1994) 3670–3674.
[7] S.T. Olson, R. Swanson, D. Day, I. Verhamme, J. Kvassman, J.D. Shore, Resolution of Michaelis complex, acylation, and conformational change steps in the reactions of the serpin, plasminogen activator inhibitor-1, with tissue plasminogen activator and trypsin, Biochemistry 40 (2001) 11742–11756.
[8] J.O. Kvassman, I. Verhamme, J.D. Shore, Inhibitory mechanism of serpins: loop insertion forces acylation of plasminogen activator by plasminogen activator inhibitor-1, Biochemistry 37 (1998) 15491–15502.
[9] G.E. Blouse, M.J. Perron, J.O. Kvassman, S. Yunus, J.H. Thompson, R.L. Betts, et al., Mutation of the highly conserved tryptophan in the serpin breach region alters the inhibitory mechanism of plasminogen activator inhibitor-1, Biochemistry 42 (2003) 12260–12272.
[10] E.L. Madison, E.J. Goldsmith, R.D. Gerard, M.J.H. Gething, J.F. Sambrook, R.S. Basselduby, Amino-acid-residues that affect interaction of tissue-type plasminogen-activator with plasminogen-activator inhibitor-1, Proc. Natl. Acad. Sci. USA 87 (1990) 3530–3533.
[11] C.A. Ibarra, G.E. Blouse, T.D. Christian, J.D. Shore, The contribution of the exosite residues of plasminogen activator inhibitor-1 to proteinase inhibition, J. Biol. Chem. 279 (2004) 3643–3650.
[12] K. Tachias, E.L. Madison, Variants of tissue-type plasminogen activator that display extraordinary resistance to inhibition by the serpin plasminogen activator inhibitor type 1, J. Biol. Chem. 272 (1997) 14580–14585.
[13] Q. Wang, S. Shaltiel, Distal hinge of plasminogen activator inhibitor-1 involves its latency transition and specificities toward serine proteases, BMC Biochem. 4 (2003) 5.
[14] P.M. Sherman, D.A. Lawrence, I.M. Verhamme, D. Paielli, J.D. Shore, D. Ginsburg, Identification of tissue-type plasminogen activator-specific plasminogen activator inhibitor-1 mutants. Evidence that second sites of interaction contribute to target specificity, J. Biol. Chem. 270 (1995) 9301–9306.
[15] R.J. Dekker, A. Eichinger, A.A. Stoop, W. Bode, H. Pannekoek, A.J. Horrevoets, The variable region-1 from tissue-type plasminogen activator confers specificity for plasminogen activator inhibitor-1 to thrombin by facilitating catalysis: release of a kinetic block by a heterologous protein surface loop, J. Mol. Biol. 293 (1999) 613–627.
[16] M.J. Perron, G.E. Blouse, J.D. Shore, Distortion of the catalytic domain of tissue-type plasminogen activator by plasminogen activator inhibitor-1 coincides with the formation of stable serpin–proteinase complexes, J. Biol. Chem. 278 (2003) 48197–48203.
[17] A. Vindigni, M. Winfield, Y.M. Ayala, E. Di Cera, Role of residue Y99 in tissue plasminogen activator, Protein Sci. 9 (2000) 619–622.
[18] E.L. Madison, E.J. Goldsmith, R.D. Gerard, M.J. Gething, J.F. Sambrook, Serpin-resistant mutants of human tissue-type plasminogen activator, Nature 339 (1989) 721–724.
[19] L.H. Gong, M. Liu, T. Zeng, X.L. Shi, C. Yuan, P.A. Andreasen, et al., Crystal structure of the Michaelis complex between tissue-type plasminogen activator and plasminogen activators inhibitor-1, J. Biol. Chem. 290 (2015) 25795–25804.
[20] Z. Lin, L. Jiang, C. Yuan, J.K. Jensen, X. Zhang, Z. Luo, et al., Structural basis for recognition of urokinase-type plasminogen activator by plasminogen activator inhibitor-1, J. Biol. Chem. 286 (2011) 7027–7032.
[21] M.B. Berkenpas, D.A. Lawrence, D. Ginsburg, Molecular evolution of plasminogen-activator inhibitor-1 functional stability, EMBO J. 14 (1995) 2969–2977.
[22] J.K. Jensen, T. Wind, P.A. Andreasen, The vitronectin binding area of plasminogen activator inhibitor-1, mapped by mutagenesis and protection against an inactivating organochemical ligand, FEBS Lett. 521 (2002) 91–94.
[23] D.M. Dupont, J.B. Madsen, T. Kristensen, J.S. Bodker, G.E. Blouse, T. Wind, et al., Biochemical properties of plasminogen activator inhibitor-1, Front. Biosci. 14 (2009) 1337–1361.
[24] J.A. Huntington, Shape-shifting serpins – advantages of a mobile mechanism, Trends Biochem. Sci. 31 (2006) 427–435.
[25] B. Van de Craen, P.J. Declerck, A. Gils, The biochemistry, physiology and pathological roles of PAI-1 and the requirements for PAI-1 inhibition in vivo, Thromb. Res. 130 (2012) 576–585.
[26] M. Schnolzer, P. Jedrzejewski, W.D. Lehmann, Protease-catalyzed incorporation of O-18 into peptide fragments and its application for protein sequencing by electrospray and matrix-assisted laser desorption/ionization mass spectrometry, Electrophoresis 17 (1996) 945–953.
[27] Z. Otwinowski, W. Minor, Processing of X-ray diffraction data collected in oscillation mode, Macromol. Crystallogr. Pt A 276 (1997) 307–326.
[28] A. Vagin, A. Teplyakov, MOLREP: an automated program for molecular replacement, J. Appl. Crystallogr. 30 (1997) 1022–1025.
[29] M. Renatus, W. Bode, R. Huber, J. Sturzebecher, D. Prasa, S. Fischer, et al., Structural mapping of the active site specificity determinants of human tissue-type plasminogen activator – implications for the design of low molecular weight substrates and inhibitors, J. Biol. Chem. 272 (1997) 21713–21719.
[30] T.J. Stout, H. Graham, D.I. Buckley, D.J. Matthews, Structures of active and latent PAI-1: a possible stabilizing role for chloride ions, Biochemistry 39 (2000) 8460–8469.
[31] G.N. Murshudov, A.A. Vagin, E.J. Dodson, Refinement of macromolecular structures by the maximum-likelihood method, Acta Crystallogr. Sect. D – Biol. Crystallogr. 53 (1997) 240–255.
[32] P. Emsley, K. Cowtan, Coot: model-building tools for molecular graphics, Acta Crystallogr. Sect. D – Biol. Crystallogr. 60 (2004) 2126–2132.
[33] R.A. Laskowski, M.W. Macarthur, D.S. Moss, J.M. Thornton, Procheck – a program to check the stereochemical quality of protein structures, J. Appl. Crystallogr. 26 (1993) 283–291.
[34] L. Schrodinger, 2010. The PyMOL molecular graphics system, version 1.3 r1. There is no corresponding record for this reference.
[35] E. Krissinel, K. Henrick, Inference of macromolecular assemblies from crystalline state, J. Mol. Biol. 372 (2007) 774–797.